2015 15th International Conference on Control, Automation and Systems (ICCAS 2015)
Oct. 13-16, 2015 in BEXCO, Busan, Korea

Energy Conversion
Circuit Laboratory

Analysis and Control of Capacitive-coupled Wireless Power Transmission System

Hee-Su Choi, Jun-Young Park, and Sung-Jin Choi*

School of Electrical Engineering, University of Ulsan,
Ulsan, 680-749, Korea (sjchoi@ulsan.ac.kr) * Corresponding author

Abstract: Electric field-coupled wireless power transmission utilizes the electric field applied between the physically separated metal plates. In this application, how to provide the regulated output voltage through the resonant LC link are challenging task. In this paper, analysis and control design of such system are investigated. Following small signal and high Q approximation, transfer function of the overall power stage including the transmitter and receiver circuit is extracted and the control loop is designed in the frequency domain. The theoretical results are verified by PSIM simulation for a 10V/0.5A prototype system.

Keywords: wireless power transmission, capacitive coupling, coupled electric field, resonant converter

1. INTRODUCTION

Capacitively-coupled wireless power transmission (CPT) utilizes the electric field applied between the physically separated metal barriers. The link capacitance formed between both sides of the barrier is a doubled-edged sword because it not only provides the ac current path through the barrier but also decreases the power factor and thus deteriorates the power transfer efficiency of the overall system.

In order to cancel out the capacitance to improve the efficiency, many researches has been performed and they add extra inductive reactance in series with the link capacitor and drive the transmitter circuit resonantly [1]. However, most of the works are about the circuit topology and there are few works on its control issue. The reason is because they consider only battery charging application, but it does not cover all aspects of emerging wireless power technology.

Actually, wireless power application can be divided into two categories. First one is hybrid wireless power system which admits intermittent power transmission because the receiving object has a sufficient battery energy supply in it. Applications such as charging stations for cell phones, vacuum cleaners, or robots fall into this group. In this case, battery itself has a large time constant inherited from chemical reaction and does not need fast control. It needs just flow control of charging sequence between the constant current / constant voltage (CC/CV) modes whose time constants are more than a few tens of minutes [2,3].

On the contrary, the other application which needs continuous power transmission through the wireless energy link can be categorized as full wireless power system. It has no battery inside the target object. Therefore, regulating the output voltage in the receiving circuit are challenging task to be investigated. Moreover, because the transmitter and receiver are physically separated, the control loop should be implemented by the wireless feedback link. In this paper, a surface wireless power system based on coupled electric field is analyzed and small signal modeling of the overall power stage is performed. In order to obtain the regulated output voltage in the absence of battery power in the target object, the guideline for the control loop implementation is also presented.

2. SYSTEM DESCRIPTION

Figure 1 shows the block diagram of the target system. It consists of transmitter, receiver, energy link, and the control circuitry. From the dc input voltage, transmitter provides the high frequency ac voltage waveforms to the energy link and the receiver rectifies the ac waveforms and restores the dc voltage with a pre-determined dc voltage gain.

The dotted line in the center of the figure depicts the physical barrier between the transmitter and the receiver. The system contains two separate energy link locations and they provide the link capacitances which admit high frequency currents to flow through them. Each link capacitance can be formed by a pair of metal structure in any shape like plane, cylinder, or sphere etc. For example, if a pair of square plates with dimension of 10cm x 10cm separated by 0.15mm air gap constitutes about 500pF. Considering the two locations of the energy link, the effective link capacitance is the series combination of those two capacitances and is almost half of each capacitance value.

The most appropriate circuit topology is the half

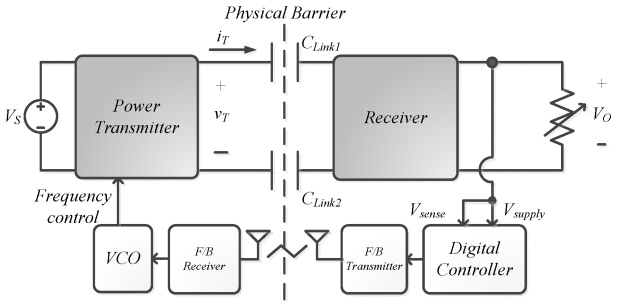

Fig. 1 Full wireless power system based on CPT

978-89-93215-09-0/15/$31.00 ©ICROS

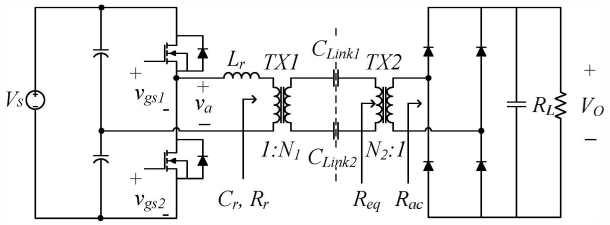

Fig. 2 Power stage topology for CPT

bridge structure with double matching transformers which was proposed in [4] and is shown in Fig. 2. In this configuration, transmitter contains two power MOSFETs turning on alternatively with 50% duty cycle to provide the ac voltage waveforms. The series inductor, L_r, is introduced to compensate the reactance of the effective link capacitance, C_e. The input transformer, TX1 provides the impedance matching to provide zero voltage turn-on features to the main switches and minimizes the switching loss. Meanwhile, the resonant waveforms are restored to dc voltage by the full-wave rectifier on the load resistance, R_L, and output filter capacitor, C_f, in the receiver circuit. The output matching transformer, TX2 is adopted to increase the effective output load impedance seen by LC resonant tank.

3. POWER STAGE MODELING

3.1 Power stage

1) DC characteristics

To analyze the power stage, starting point will be obtaining dc voltage transfer gain. Because power conversion takes advantage of the resonant characteristics of the LC series tank, it is possible to assume the fundamental harmonic approximation techniques given in [5] and simple circuit analysis produces the output voltage, vo, given by the following relation.

$$v_O = N \cdot m(q, f_N) \cdot v_G \tag{1}$$

The v_G is the half of the input voltage, N is the overall transformer turn ratio, and $m(\cdot)$ is the gain function given by

$$N = \frac{N_1}{N_2} \tag{2}$$

and

$$m(q, f_N) = \left\{ 1 + q^2 \left(f_N - \frac{1}{f_N} \right)^2 \right\}^{-\frac{1}{2}}. \tag{3}$$

In this equation, q is the load function which is commonly named as load quality factor and f_N is the relative frequency ratio between the switching frequency, f_s, and the resonant frequency, F_o, of the LC tank. Eqs. (4) to (6) define those quantities.

$$q = \frac{\pi^2}{8 N^2 R_L} \sqrt{\frac{N_1^2 L_r}{Ce}} \tag{4}$$

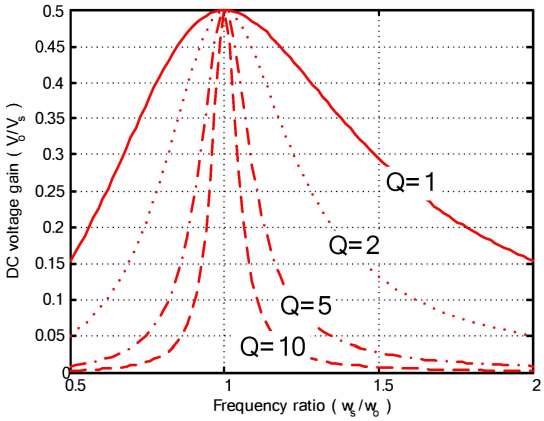

Fig. 3 Characteristics of gain function, $m(q, f_N)$

$$f_N = \frac{f_s}{F_O} \tag{5}$$

$$F_O = \frac{1}{2\pi\sqrt{N_1^2 L_r C_e}}. \tag{6}$$

As shown in Fig. 3, the gain function depends heavily on the switching frequency and the load quality factor. The dependency indicates that, in order to regulate the output voltage despite of the disturbances in the input voltage and the load, the switching frequency itself is the control variable that can be used in feedback control.

2) Low frequency characteristics

With small signal assumption, introducing Taylor series expansion up to the first derivative decomposes the system input and output variables as follows.

$$\begin{aligned} v_G &= V_G + \hat{v}_g \\ i_O &= I_O + \hat{i}_o \\ q &= Q_O + \hat{q} \\ f_S &= F_S + \hat{f}_s \\ v_O &= V_O + \hat{v}_o \end{aligned} \tag{7}$$

The first term in Eq. (7) denotes the bias point and the second term is the differential term.

Applying partial differentiation on Eq. (1), the differential output voltage is represented as

$$\hat{v}_o = \frac{\partial v_O}{\partial v_G}\hat{v}_g - \frac{\partial v_O}{\partial i_O}\hat{i}_o + \frac{\partial v_O}{\partial f_N}\frac{\partial f_N}{\partial f_S}\hat{f}_s. \tag{8}$$

The individual multiplier in each term in Eq. (8) is the differential gain evaluated on the bias condition, and will be referred as $G_{vg,0}$, $Z_{vi,0}$, and $G_{vf,0}$ respectively.

$$G_{vg,0} = N \cdot m(Q, F_n) \tag{9}$$

$$Z_{vi,0} = R_L Q^2 \left(F_n - \frac{1}{F_n} \right)^2 \tag{10}$$

$$G_{vf,0} = -\frac{N V_G Q^2}{F_O} \left(F_n - \frac{1}{F_n} \right) \left(1 + \frac{1}{F_n^2} \right) \left\{ 1 + Q^2 \left(F_n - \frac{1}{F_n} \right)^2 \right\}^{-\frac{3}{2}} \tag{11}$$

The above equations are derived from Eq. (1) which assumes power balance and thus are valid only up to the frequency range where the output filter does not start to prevail.

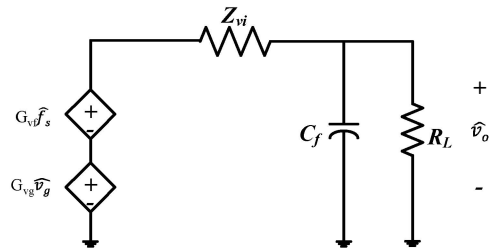

Fig. 4. Small signal equivalent circuit

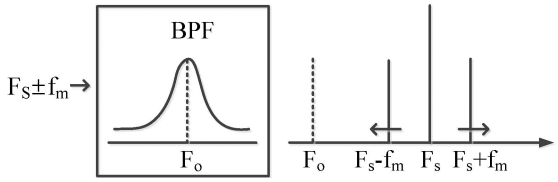

Fig. 5. Frequency modulation and beat frequency

3) High frequency characteristics

Figure 4 shows the equivalent circuit including the output filter dynamics. By the circuit time constant analysis, we can know that there exits low pass filter which generates single pole in the following location.

$$f_{pf} = \frac{1}{2\pi C_f (R_L \,||\, Z_{vi})} \tag{12}$$

Moreover, the LC resonant tank acts as a high pass filter and generates an additional two more pole into the system which is given by the beat frequency between the bias switching frequency, F_s, and the resonant frequency, F_o [6]. For example, when the switching frequency is perturbed with a modulation frequency, f_m (f_m>0), there will be a side band in the response of the driving frequency and resonance phenomenon occurs in the additional natural frequency, f_{pn}, given by

$$f_{pn} = F_S - F_O \cdot \tag{13}$$

Thus, control to output transfer function $G_{vf}(s)$ is given by

$$G_{vf}(s) = G_{vf,o} \frac{1}{\left(1+\frac{s}{\omega_{pf}}\right)\left(1+\frac{s}{Q_O\omega_{pn}}+\frac{s^2}{\omega_{pn}^2}\right)} \tag{14}$$

where ω_{pf} and ω_{pn} are the angular frequencies of the corresponding pole locations. If F_s is well above F_o, the system can be approximated as a first order system. The dominant pole assumption fails if F_s is very close to F_o.

3.2 Control loop design guideline

The control block diagram of the overall power stage is shown in Fig. 6. In the figure, K_V is the feedback sensing gain and K_{VCO} is the gain in the voltage controlled oscillator and C(s) is the compensator block to be designed here. The loop gain of the negative feedback system is

$$T(s) = K_{VCO} \cdot K_V \cdot G_{vf}(s) \cdot C(s) \tag{15}$$

If the switching frequency is well above the resonant

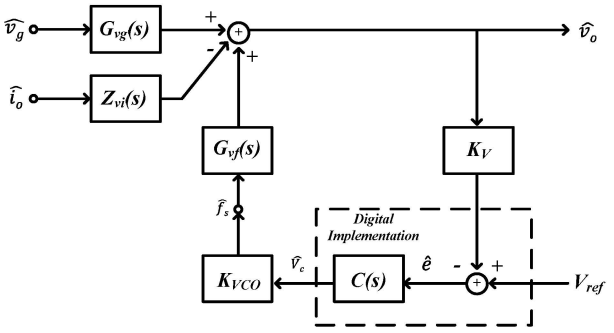

Fig. 6 Control block diagram

frequency and the bias load quality factor, Q_O is sufficiently high, proportional-integral (PI) controller,

$$C(s) = k_p + \frac{k_i}{s} \tag{16}$$

where k_p and k_i are proportional and integral coefficients, can be designed by the following design guideline. At first, the first compensator zero is placed at the low frequency output filter pole to cancel out the power stage pole in the following way.

$$\frac{k_i}{k_p} = \frac{1}{(R \,||\, Z_{vi})C_f} \tag{17}$$

Then the control loop bandwidth frequency is placed well below f_{pn} to prevent additional phase lag and avoid conditional stability situation which may deteriorate the phase margin in the loop gain. If the control loop crossover frequency, f_c (<<f_{pn}) is selected, the following condition holds.

$$\left|T(j2\pi f_c)\right| = K_{VCO} \cdot K_V \cdot G_{vf,0} \cdot k_i \frac{1}{2\pi f_c} = 1 \tag{18}$$

Therefore, combining Eq. (17) and Eq. (18), k_p and k_i can be determined. In this case, both are negative numbers.

4. VERIFICATION

Figure 7 is the implementation of CPT system in PSIM circuit simulator [7]. The power stage is designed to transmit 5W power through a pair of square plates with dimension of 10cm x 10cm separated by 0.15mm air gap and supplies the output voltage of 10V up to 0.5A load current. Table 1 shows the parameters used in the system construction.

The theoretical study on the power stage transfer

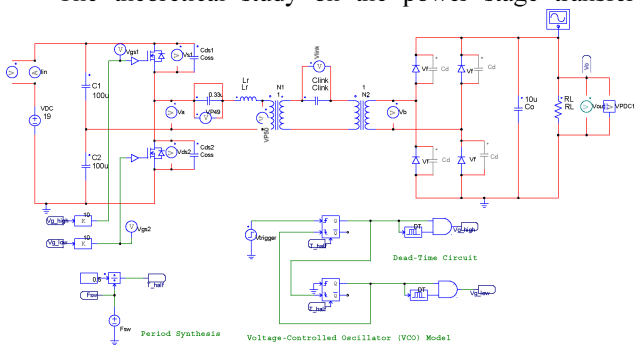

Fig. 7 Simulation setup

Table 1 System parameters

V_S	19V	V_G	9.5V
C_e	256pF	I_O	0.5A
L_r	23uH	Q_O	10Ω/ Ω
N_1	9.0	F_S	250kHz
N_2	3.9	V_O	10V
C_f	10uF	F_O	230kHz
K_{VCO}	57kHz/V	K_V	0.1V/V

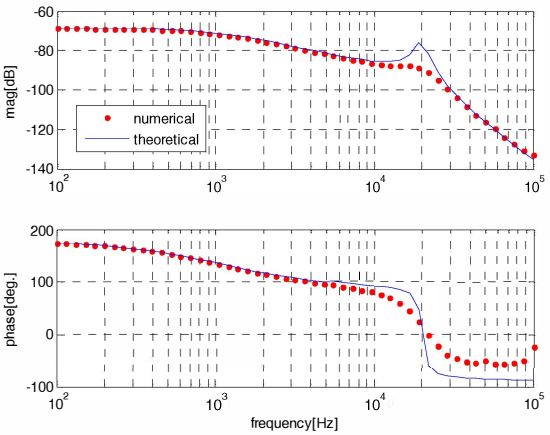

Fig. 8 Control to output transfer function, Gvf(s)

function given by Eq. (14) predicts that the low frequency pole and the high frequency natural poles exit in 1.07kHz and 20kHz, respectively. Fig. 8 shows the comparison between the theoretical analysis and numerical calculation results performed by the swept sine analysis on the PSIM circuit simulator and two graphs show good agreement. Moreover, the resonant frequency and operating frequency are well separated and the power system can be approximated by the dominant pole approximation. Therefore, the controller design approach explained in the previous section can be directly applied to this system.

Solving Eq. (17) and Eq. (18) with f_c=2kHz, k_i =-5700, k_p=-0.86 are obtained. Fig. 9 shows the Nyquist plot of the loop gain including the PI controller that has been designed. The compensator provides the phase margin of 60 degree and gain margin of 10dB to the power stage at the full load condition. Fig. 10 shows the step response when the load current is slightly increased by 10% and then decreased by 10% from the 0.5A full load condition, and the system shows good performance in the output regulation.

5. CONCLUSIONS

This paper analyzed the power stage of the CPT system which involves resonant LC link to transmit power through the physically isolated metal barrier. Applying small signal and high Q approximation to the double matched half-bridge power stage which is widely accepted in this application, it is shown that the

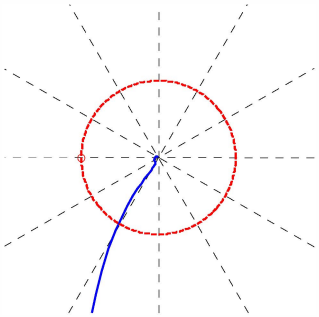

Fig. 9 Nyquist diagram of T(s)

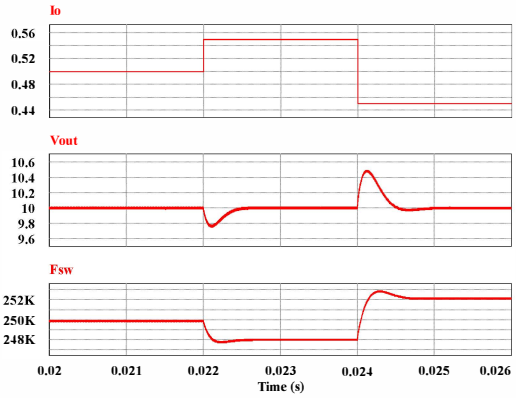

Fig. 10 Output voltage regulation when load changes

power stage transfer function is modeled as a three-pole system and can be further simplified into a single-pole system when the switching frequency and the resonant frequency are well separated. The theoretical results are successfully verified by PSIM simulation for a 10V/0.5A prototype system. Moreover, the control loop design by the suggested guideline shows good performance even in the disturbance. Because the transmitter and receiver are physically separated, the control loop should be implemented wirelessly and thus the effect of the wireless control link will be included in the subsequent work that is still under study.

REFERENCES

[1] C. Liu, A. P. Hu, and N. K. C. Nair, "Modelling and analysis of a capacitively coupled contactless power transfer system," *IET Power Electronics*, vol. 4, no. 7, pp. 808-815, 2011.

[2] Wireless Power Consortium, *The Qi Interface Specification Volume I : Low Power*, 2010.

[3] C.-G. Kim, D.-H. Seo, J.-S. You, J.-H. Park, and Bo H. Cho, "Design of a Contactless Battery Charger for Cellular Phone," *IEEE Transactions on Industrial Electronics*, vol. 48, no. 6, pp. 1238-1247, Dec. 2001.

[4] S.-J. Choi, S.-Y. Kim, and B.-W. Choi, "Power Stage Design for a Surface Wireless Power Transmission System using a Coupled Electric Field," *Journal of Institute of Control, Robotics*

and Systems, vol. 20, no. 2, pp. 143-148, 2014.

[5] R. L. Steigerwald, "A comparison of half-bridge resonant converter topologies," *IEEE Transactions on Power Electronics*, vol. 3, no. 2, pp. 174-182, Apr. 1988.

[6] V. Vorperian, "Approximate Small-Signal Analysis of the Series and the Parallel Resonant Convertes," *IEEE Transactions on Power Electronics*, vol. 4, no. 1, Jan. 1989.

[7] Powersim, *PSIM User's guide ver. 9*, May 2012.